JOURNAL OF SOLID STATE CHEMISTRY 103, 307–313 (1993)

Superconductivity in the A_xNbS_2 Intercalation Compounds (A = Cs, Rb)

BAI-HAO CHEN,* BRYAN EICHHORN,* JIAN-LIANG PENG,† AND RICHARD L. GREENE†

*Center for Superconductivity Research, Departments of *Chemistry and †Physics, University of Maryland, College Park, Maryland 20742*

Received May 27, 1992; in revised form July 31, 1992; accepted August 3, 1992

Four new A_xNbS_2 phases, where A = Cs, x = 0.34, 0.60; A = Rb, x = 0.33, 0.6, were prepared from Nb and A_2CO_3, in a CS_2/Ar atmosphere at 700°C. The compounds were refined (Rietveld profile analysis) in $P6_3/mmc$ symmetry. Crystal data were $Cs_{0.34}NbS_2$, a = 3.3452(5) Å, c = 18.424(5) Å; $Cs_{0.60}NbS_2$, a = 3.3539(6) Å, c = 18.324(1) Å; $Rb_{0.33}NbS_2$, a = 3.3425(5) Å, c = 18.075(2) Å; $Rb_{0.6}NbS_2$, a = 3.3462(3) Å, c = 17.986(2) Å. The compounds comprise a $2H$-NbS_2 host with trigonal prismatic Nb ions and alkali ions intercalated in trigonally distorted octahedral holes between NbS_2 layers. Increasing the alkali content effects a decrease in the c lattice parameters due to decreases in *inter*layer S···S separations. Magnetic susceptibility and resistivity measurements indicate metallic behavior for all compounds below room temperature. The Cs phases are bulk type II superconductors ($Cs_{0.34}NbS_2$, T_c = 3.0 K, $Cs_{0.60}NbS_2$, T_c = 2.0 K).

Introduction

The chemistry and physics of the layered transition metal dichalcogenides of formula MQ_2 (where M is a group 4, 5, or 6 transition metal and Q is S, Se, Te) have been studied extensively and are the subject of several reviews (*1–4*). Initial interest in these materials stemmed from the discovery of superconductivity in the MQ_2 compounds and their organic and inorganic derivatives. In particular, the MQ_2 sulfides and selenides of Nb and Ta are low temperature superconductors with transition temperatures (T_c) ranging from 7.2 K for $2H$-$NbSe_2$ to 0.15 K for $2H$-$TaSe_2$ (*4*). The transition temperature for $2H$-NbS_2 is 6.2 K (*5*).

Several generalizations can be made concerning superconductivity in the MQ_2 materials (M = Nb, Ta) and their intercalation compounds. (1) Superconductivity is most often observed with trigonal prismatic coordination of the group 5 metal. The MQ_2 polymorphs with octahedrally coordinated metals are not normally superconducting before or after intercalation (*4*). (2) Intercalation of donor organic molecules shifts the value of T_c but does not destroy superconductivity in the MQ_2 host (*3, 6*). (3) Intercalation of transition elements or post-transition elements into NbS_2 and MSe_2 destroys superconductivity of the MQ_2 host (*4, 7*). The exceptions are the Bi_xTaS_2 and stoichiometric $ATaS_2$ phases (A = Hg, In, Sn, Pb) which are superconducting between 0.5 and 3 K (*8*). (4) Superconductivity is preserved in intercalated, hydrated alkali metal complexes (*9*) of formula $(A_x)^{x+}(H_2O)_y[TaS_2]^{x-}$

0022-4596/93 $5.00

but is destroyed in the nonhydrated alkali metal phases of niobium and tantalum (A_xMQ_2 where A = Li, Na, K and $0 \leq x \leq 1$) (*1, 9–11*). Interestingly, alkali intercalation induces superconductivity in the semiconducting MQ_2 phases of Mo and Zr with the highest T_c's associated with the Cs and Rb phases [$Cs_{0.3}MoS_2$ and $Rb_{0.3}MoS_2$, T_c = 6.9 K] (*4, 10, 12*). To our knowledge, the preparation and properties of the Cs and Rb phases of the group 5 dichalcogenides have not previously been reported.

We report here the preparation, structure, and properties of the Cs_xNbS_2 and Rb_xNbS_2 phases where $0.3 \leq x \leq 0.6$. Unlike the other A_xMS_2 phases where M = Nb, Ta, the Cs_xNbS_2 phases are bulk superconductors.

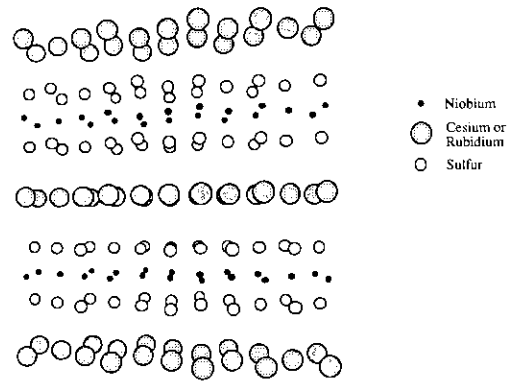

FIG. 1. Ball drawing of the A_xNbS_2 phases (A = Rb, Cs) showing the intercalated A^+ ions between the NbS_2 layers.

Experimental

The A_xNbS_2 phases were prepared from stoichiometric ratios of A_2CO_3 and Nb metal precursors (Cerac Inorganics) fired at 700°C for two days under a flowing Ar/CS_2 atmosphere. The resulting materials were homogeneous black microcrystalline powders that appeared to be single phase by powder X-ray diffraction (XRD). Atomic absorption analyses (AA) were conducted by Schwarzkopf Microanalytical Laboratories, Woodside, NY.

The X-ray data were collected on a modified Phillips XRG 2000 diffractometer ($CuK\alpha$ radiation) interfaced with a RADIX databox and an MDI software system. Data were collected at 0.02° intervals with 20-sec count rates and refined by Rietveld analysis (Micro-Riet, MDI) on a Compuadd 386 personal computer. The A_xNbS_2 phases were successfully refined under hexagonal symmetry (space group $P6_3/mmc$) with Pearson VII profile shape functions. Preferred orientation was treated using the March function (*13*) as defined by

$$G_{hkl} = (G_1^2\cos^2\alpha + G_1^{-1}\sin^2\alpha)^{-3/2},$$

where G_1 is the preferred orientation parameter and α is the acute angle between the scattering vector and the normal to the plane of the crystallites. The refinement data are summarized in Table I.

Magnetic susceptibilities of the A_xNbS_2 compounds were carried out on finely ground powders of single phase samples by using a Quantum Design Superconducting Quantum Interface (SQUID) Magnetometer at applied fields of 1–30,000 Oe. Standard four-probe resistivity experiments were conducted on sintered polycrystalline samples.

Results and Discussion

The A_xNbS_2 compounds crystallize in the hexagonal space group $P6_3/mmc$ and display significant preferred orientations along $00l$. The structures of the Cs_xNbS_2 compounds, where x = 0.34 and 0.60, were successfully refined in one of the four A_xNbS_2 models (the α-model) proposed for the Na and K phases by Omloo and Jellinek (*11*). Attempted refinements using the other models were not successful. A schematic drawing of the structures is shown in Fig. 1 and the calculated and observed X-ray diffraction data for the $Cs_{0.60}NbS_2$ phase are shown

TABLE I

CRYSTALLOGRAPHIC DATA FOR THE A_xNbS_2 PHASES (A = Cs, Rb)[a]

	$Cs_{0.34}NbS_2$	$Cs_{0.60}NbS_2$	$Rb_{0.33}NbS_2$	$Rb_{0.6}NbS_2$
a(Å)	3.3425(5)	3.3539(6)	3.3425(5)	3.3462(3)
c(Å)	18.424(5)	18.324(1)	18.075(2)	17.986(2)
c/a	5.51	5.46	5.41	5.38
Volume (Å^3)	178.15(4)	178.51(5)		
Density (g/cm^3)	3.766	4.368		
R (%)[b]	7.45	9.22[c]		
R_{wp} (%)[b]	7.24	13.31[c]		
R_{Bragg} (%)[b]	7.54	6.57[c]		
Cs occupation	0.34	0.60		
z fractional coordinate for sulfur[d]	0.165	0.159		

[a] Space group $P6_3/mmc$.

[b] $R = \{[\Sigma_i(I_i^{obs} - I_i^{calc})^2]/[\Sigma(I_i^{obs})^2]\}^{1/2}$. $R_{wp} = \{[\Sigma_i w_i(I_i^{obs} - I_i^{calc})^2]/[\Sigma w_i(I_i^{obs})^2]\}^{1/2}$. $R_{Bragg} = [\Sigma_i|F_i^{obs} - F_i^{calc}|]/[\Sigma_i F_i^{obs}]$.

[c] Some atoms non-positive definite in final cycles of refinement.

[d] Fractional coordinates are Cs—0, 0, 0; Nb—0, 0, $\frac{1}{4}$; S—$\frac{1}{3}$, $\frac{2}{3}$, z.

in Fig. 2. The refined occupation of Cs in this phase (x = 0.34) was in excellent agreement with the AA results which yielded a Cs : Nb ratio of 0.36 : 1.0. The $Cs_{0.60}NbS_2$ compound and two other Rb phases, $Rb_{0.33}NbS_2$ and $Rb_{0.6}NbS_2$, were refined to give reasonable R factors and profile fits, but perhaps due to the preferred orientations, some negative thermal parameters were observed in the final cycles of refinement. Despite the re-

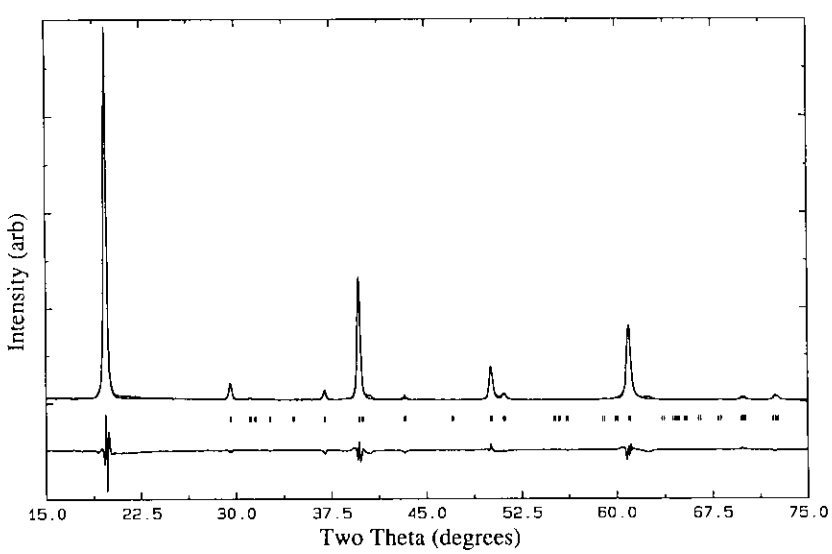

FIG. 2. Rietveld profile analysis of the $Cs_{0.60}NbS_2$ phase showing the observed (points) and calculated (solid line) profiles with the difference profile (lower, same scale).

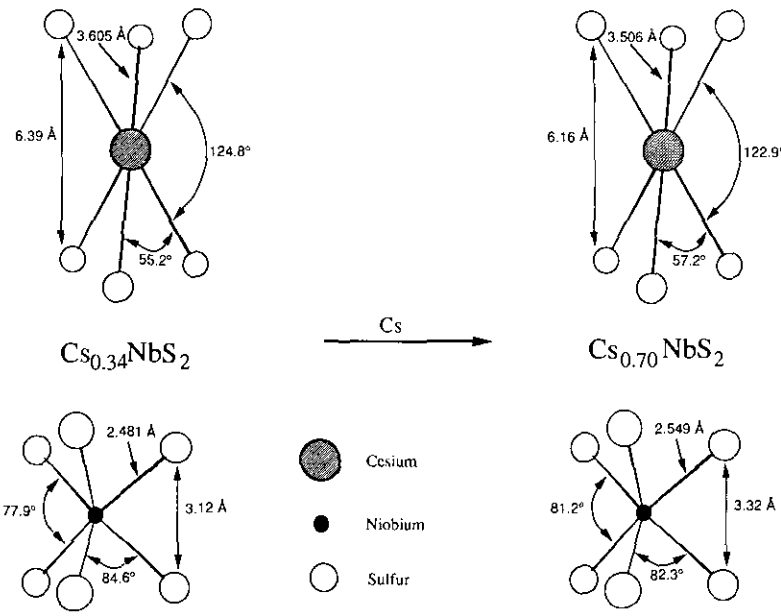

FIG. 3. Schematic drawings of the NbS_6 and CsS_6 coordination environments in the $Cs_{0.34}NbS_2$ and $Cs_{0.60}NbS_2$ phases. Pertinent bond distances and angles are shown for comparison.

finement difficulties associated with the latter phases, the resulting atomic coordinates, bond distances, and bond angles were quite reasonable. The structural parameters for the Cs compounds are listed in Table II. A comparison of the $x = 0.34$ and $x = 0.60$ members of the Cs_xNbS_2 phases is given in Fig. 3.

TABLE II

INTERATOMIC DISTANCES (Å) AND ANGLES (°) FOR THE Cs_xNbS_2 PHASES

	Cs(0.34)	Cs(0.60)
Cs–S	3.605 (9)	3.506 (9)
Nb–S	2.481 (7)	2.549 (7)
S···S (Nb)	3.12 (2)	3.32 (2)
S···S (Cs)	6.39 (2)	6.16 (1)
S–Cs–S	55.2 (1)	57.2 (1)
S–Cs–S'	124.8 (8)	122.9 (5)
S–Nb–S	77.9 (6)	81.2 (6)
S–Nb–S'	84.6 (2)	82.3 (2)

The structure of $Cs_{0.34}NbS_2$ consists of a $2H$-NbS_2 host (*1*) with trigonally distorted octahedral Cs^+ ions (trigonal antiprismatic) intercalated between the NbS_2 layers. The Cs–S contacts are quite long at 3.605 (*9*) Å. The Nb atoms are trigonal prismatic with Nb–S contacts of 2.481 (*7*) Å which are similar to the 2.47 Å contacts of NbS_2 (*14*).

In the $Cs_{0.60}NbS_2$ phase, the higher Cs content results in additional electron transfer into the NbS_2 "d_{z^2} conduction band" (*3*, *8*). Because the d_{z^2} conduction band appears to be localized on Nb, additional filling of this band formally reduces the Nb oxidation state thereby generating a larger effective Nb atomic radius. The covalent nature of the Nb–S bonding should also affect a slight increase in the effective radius of sulfur. As expected, the Nb–S contacts are longer in $Cs_{0.60}NbS_2$ at 2.549 (7) Å in comparison to those of $Cs_{0.34}NbS_2$. This Nb–S bond elongation effects a slight increase in the a lattice parameter and an increase in the separation

between the sulfide layers hosting the Nb atoms (Fig. 3). In contrast, the Cs–S distances of 3.506 (9) Å are significantly shorter than the corresponding 3.605 (9) Å contacts in $Cs_{0.34}NbS_2$ which presumably results from decreased coulombic repulsions due to intercalation of additional Cs^+ ions between the negatively charged sulfide layers (*1*, *4*). The Cs–S bond contraction allows for a large decrease in the S···S contacts between NbS_2 layers from 6.39 (2) Å in $Cs_{0.34}NbS_2$ to 6.16 (1) Å in $Cs_{0.60}NbS_2$ (Fig. 3). This large decrease in *inter*layer S···S separation overcompensates for the increase in the *intra*layer separation and is responsible for the decrease in the c lattice parameter.

Resistivity measurements showed metallic behavior below room temperature for $Cs_{0.34}NbS_2$, $Cs_{0.60}NbS_2$, $Rb_{0.33}NbS_2$, and $Rb_{0.6}NbS_2$. Normal state dc susceptibilities of the samples were determined by cooling the samples to 4 K, applying a 30-kOe field, and measuring the magnetization periodically as the temperature was slowly raised to 350 K over a 10-hr period. The samples showed small, roughly temperature independent paramagnetic signals from 350 to 80 K with Curie tails below 80 K due to a small concentration of $S = \frac{1}{2}$ magnetic impurities. After fitting and subtracting the impurity contributions, the susceptibilities were essentially temperature independent. The susceptibility for $Cs_{0.34}NbS_2$ above 4 K is shown in Fig. 4 and a summary of the room temperature susceptibilities (χ_0 values) is given in Table III. These samples show small but reproducible "spikes" between 40 and 60 K which we (*15*) and others (*16*) have observed in related Ba and Sr layered niobium sulfide phases. The origin of this anomaly is not known at present.

The low temperature dc susceptibilities (2-Oe field) of the Cs_xNbS_2 phases show diamagnetic signals below 3 K indicating the onset of superconductivity. The onset temperatures and superconducting fractions associated with these phases are summarized

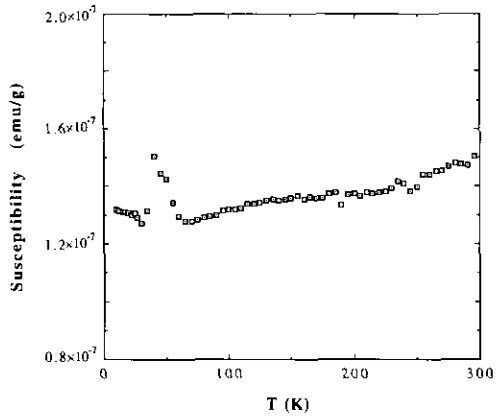

FIG. 4. Plot of magnetic susceptibility versus temperature between 350 and 4 K for $Cs_{0.34}NbS_2$. The experiments were conducted in a 30-kOe field.

in Table III. The shielding (zero field cooled) and Meissner (field cooled) fractions for $Cs_{0.60}NbS_2$ are 94% and 45%, respectively, indicating bulk superconductivity. The superconducting fractions are defined as

$$\%f = \frac{4\pi M \cdot \rho}{H_{app}} \times 100,$$

where M is the magnetization (emu/g), ρ is the density (g/cm^3), and H_{app} is the applied magnetic field. The maximum T_c observed to date is 3 K found for $Cs_{0.34}NbS_2$, however, the low Meissner fraction (8%) and broad transition are indicative of an inhomogeneous sample. The field-cooled and zero-field-cooled susceptibilities of $Cs_{0.34}NbS_2$ and $Cs_{0.60}NbS_2$ are shown in Fig. 5. Attempted preparations of the $x = 0.2$ member of this series have thus far yielded heterogeneous materials (XRD) that show only trace diamagnetic signals below 2.2 K. The $Rb_{0.33}NbS_2$ phase shows trace superconductivity below 2 K with extremely low Meissner and shielding fractions. The $Rb_{0.6}NbS_2$ compound was not superconducting down to 1.8 K. The superconductivity observed in the $Rb_{0.33}NbS_2$ phase may in fact be due to superconducting impurity phases such as Cs_xNbS_2.

TABLE III

MAGNETIC AND SUPERCONDUCTIVITY PARAMETERS FOR THE A_xNbS_2 PHASES (A = Cs, Rb)

Compound	Gram χ_0^a (emu/g)	Molar χ_0^a (emu/mole)	T_c (K)	Shielding fraction (%)	Meissner fraction (%)
NbS_2[b]	—	12×10^{-5}	6.2		
$Cs_{0.2}NbS_2$[c]	—	—	2.2	6.5	0.8
$Cs_{0.34}NbS_2$	1.5×10^{-7}	3.0×10^{-5}	3.0	100	8.0
$Cs_{0.60}NbS_2$	0.9×10^{-7}	2.2×10^{-5}	2.0	94	45
$Rb_{0.33}NbS_2$	2.8×10^{-7}	5.2×10^{-5}	2.0	>0.1	>0.1
$Rb_{0.6}NbS_2$	5.2×10^{-7}	10.8×10^{-5}	N/O	—	—

[a] Room temperature data.
[b] From Refs. (*17, 18*).
[c] Nominal composition based on reagent ratios. Products not single phase.

A comparison of the molar susceptibilities (χ_m) and superconductivity onset temperatures in Nb (*17*), NbS_2 (*17, 18*), and the $Cs_x NbS_2$ phases (Table III) shows that the highest T_c and molar χ_0 values are associated with NbS_2 whereas the lowest T_c and χ_m values correspond to the $Cs_{0.60}NbS_2$ phase. The observed susceptibilities include contributions from the core diamagnetism (χ_{dia}), Pauli paramagnetism (χ_P), and Van Vleck paramagnetism (χ_V). Both χ_V and χ_P are affected by intercalation (*4*, p. 117) but, as a first approximation, we assume that most of the variation in χ_m is caused by χ_P. Since χ_P is proportional to the density of states at the Fermi surface, $N(E_F)$, the molar χ_m values should provide a rough measure of $N(E_F)$ in a related series of compounds. In the usual BCS theory, the T_c should vary with $N(E_F)$, with higher densities of states giving rise to higher transition temperatures, as is observed for the Cs_xNbS_2 series (where x = 0, 0.34, 0.60). A similar situation is found in the organic intercalation compounds (*4*, p. 117). The occurrence of maximum T_c with the Cs materials in the A_xNbS_2 series is consistent with an increased density of states due to lattice expansions (along a) and d_{z^2}

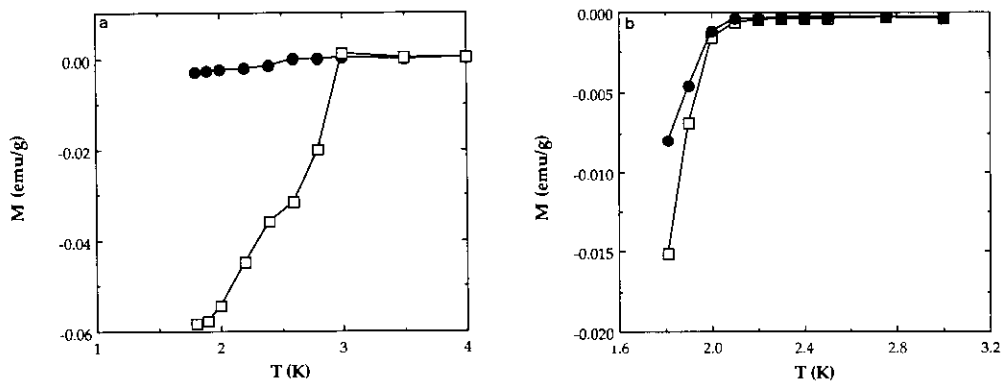

FIG. 5. Low temperature susceptibilities of the (a) $Cs_{0.34}NbS_2$ and (b) $Cs_{0.60}NbS_2$ phases recorded in a 2-Oe field. The circles and squares represent the field-cooled and zero-field-cooled data, respectively.

conduction band narrowing as has been proposed for the A_xC_{60} (*19*) family of superconductors.

In summary, the A_xNbS_2 phases (where A = Cs, Rb) comprise $2H$-NbS_2 hosts with intercalated A^+ ions occupying trigonally distorted octahedral sites between the NbS_2 layers. The octahedral coordination of the A^+ ions contrasts with the more common trigonal prismatic coordination observed in related Cs- and Rb-intercalated MS_2 phases (M = Ti, Zr, Hf, Mo, W) (*1*, *4*). In contrast to the other alkali-intercalated group 5 MS_2 phases studied to date, these materials are superconducting at low temperatures. The absence of diamagnetic signals in the low Cs content phases suggests that the superconductivity observed for the $x = 0.34$ and $x = 0.60$ Cs_xNbS_2 compounds is not merely a T_c suppressed extension of the NbS_2 host but a separate series of superconducting materials. A more detailed study of the physical properties associated with these materials is in progress and will be reported elsewhere.

Acknowledgments

This work was supported by the National Science Foundation (DMR-8913906), the Exxon Education Foundation, and the Center for Superconductivity Research and the Department of Chemistry and Biochemistry at the University of Maryland.

References

1. M. S. WHITTINGHAM, *Prog. Solid State Chem.* **12,** 41 (1978).
2. M. S. DRESSELHAUS (Ed.), "Intercalation in Layered Materials," NATO ASI Series B: Physics, Vol. 148, Plenum, New York (1986).
3. C. N. R. RAO AND K. P. R. PISHARODY, *Prog. Solid State Chem.* **10,** 207 (1976).
4. F. A. LEVY (Ed.), "Intercalated Layered Materials," Reidel, Dordrecht (1979).
5. B. W. ROBERTS, *J. Phys. Chem. Ref. Data* **5,** 581 (1976).
6. F. R. GAMBLE, J. H. OSIECKI, M. CAIS, K. R. PISHARODY, F. J. DISALVO, AND T. H. GEBALLE, *Science* **174,** 439 (1971).
7. F. HULLINGER AND E. POBITSHKA, *J. Solid State Chem.* **1,** 117 (1970).
8. F. J. DISALVO, G. W. HULL, JR., L. H. SCHWARTZ, J. M. VOORHOEVE, AND J. V. WASZCZAK, *J. Chem. Phys.* **59,** 1922 (1973).
9. (a) F. SERNETZ, A. LERF, AND R. SCHOLLHORN, *Mater. Res. Bull.* **9,** 1597 (1974); (b) A. LERF, R. SCHOLLHORN, AND F. SERNETZ, *Z. Naturforsch. B* **29,** 810 (1974); (c) R. SCHOLLHORN AND H. MEYER, *Mater. Res. Bull.* **9,** 1237 (1974).
10. (a) D. W. MURPHY, F. J. DISALVO, G. W. HULL, JR., AND J. V. WASZCZAK, *Inorg. Chem.* **15,** 19 (1976); (b) G. B. SUBBA RAO, M. W. SHAFER, AND J. C. TSANG, *J. Phys. Chem.* **79,** 553 (1975).
11. W. P. F. A. M. OMLOO AND F. JELLINEK, *J. Less-Common Met.* **20,** 121 (1970).
12. J. A. WOOLLAM AND R. B. SOMOANO, *Phys. Rev. B* **13,** 3843 (1976).
13. C. DOLLASE, *J. Appl. Crystallogr.* **19,** 1 (1986).
14. F. R. GAMBLE, *J. Solid State Chem.* **9,** 358 (1974).
15. B.-H. CHEN, B. W. EICHHORN, J. L. PENG, AND R. L. GREENE, to be published.
16. K. MATSUURA, *et al.*, *J. Solid State Chem.* **94,** 294 (1991).
17. F. KADIJK AND F. JELLINEK, *J. Less-Common Met.* **19,** 421 (1969).
18. E. I. KRYLOV, *Zh. Neorg. Khim.* **3,** 1497 (1958).
19. K. TANIGAKI, T. W. EDDESEN, S. SAITO, J. MIZUKI, J. S. TSAI, Y. KUBO, AND S. KUROSHIMA, *Nature* **352,** 222 (1991).